IEEE Access
Multidisciplinary : Rapid Review : Open Access Journal

Received December 11, 2019, accepted January 5, 2020, date of publication January 8, 2020, date of current version January 23, 2020.

Digital Object Identifier 10.1109/ACCESS.2020.2965021

Design of an Improved Implicit Generalized Predictive Controller for Temperature Control Systems

ZHENG CHEN [1], (Senior Member, IEEE), JIALUN CUI [1], ZHENZHEN LEI [2], JIANGWEI SHEN [1], AND RENXIN XIAO [1]

[1]Faculty of Transportation Engineering, Kunming University of Science and Technology, Kunming 650500, China
[2]School of Mechanical and Power Engineering, Chongqing University of Science and Technology, Chongqing 401331, China

Corresponding author: Renxin Xiao (xrx1127@foxmail.com)

This work was supported in part by the National Science Foundation under Grant 61763021 and Grant 51775063, in part by the National Key Research and Development Program of China under Grant 2018YFB0104500, and in part by the EU-Funded Marie Sklodowska-Curie Individual Fellowships Project under Grant 845102-HOEMEV-H2020-MSCA-IF-2018.

ABSTRACT In this study, an implicit proportional-integral-based generalized predictive controller (PIGPC) is proposed to effectively control temperatures of industrial systems with time-varying delay. The controller is designed to optimize the target function with the proportional-integral structure for improving the controlling performance of implicit PIGPC. Meanwhile, the recursive least square method is leveraged to directly identify the parameters of controller. Compared with the conventional implicit generalized predictive controller, the process of parameter identification converges faster. The Lagrange multiplier method is introduced to solve the optimal control law of implicit PIGPC by considering the input constraints of system. An approximate decoupling controller for multivariable systems is proposed to eliminate the coupling effects. Simulation and experimental results manifest the effectiveness and feasibility of the proposed controller in temperature control systems.

INDEX TERMS Decoupling control, input constraint, proportional-integral generalized predictive controller (PIGPC), Lagrange multiplier method, temperature control system.

I. INTRODUCTION

Temperature control plays an important role in a variety of industrial processes, such as main steam temperature system of thermal power plants and heating boilers of metallic or chemical products [1]–[3]. These thermal controlling targets usually feature unfavorable characteristics, such as nonlinearity, time-delay and time-variation, leading to design difficulty of controllers. For instance, in production process of injection molding machines, existence of multiple heating barrels gives rise to strong coupling and system uncertainty. Thus, it remains a challenging task to precisely account for the temperature control in a mathematical manner [4]. Meanwhile, system inputs may be restricted by various constraints in practical operations thanks to safety and saturation of actuators [5]. Moreover, the target temperature should be regulated quickly and precisely by effective controlling algorithms [6], and other performances such as dynamic response and low calculation effort of the controller also need to be appropriately tailored [7]. In short, the temperature system is actually a typical process optimization problem involving the reachable target, time-delay responses, time-varying constraints and proper consideration of computation intensity. An effective temperature controller is of great importance for attaining the controlling target while subject to different constraints [8].

In most cases, temperatures of industrial systems are usually regulated by proportional-integral-differential (PID) algorithms due to the ease of application [9]. However, it may result in poor dynamic response in the presence of apparent time-delay and/or unpredictable disturbances. To overcome these difficulties, a number of novel algorithms, such as Smith predictor (SP), fuzzy logic controller and neural network (NN) controller are employed in [10]–[15]. SP can effectively cope with the time-delay characteristics; however, it demands modeling the control target in a precise

The associate editor coordinating the review of this manuscript and approving it for publication was Ali Zemouche.

manner [10]. The fuzzy PID algorithm declares to improve robustness of temperature control by dynamically changing the controller's parameters online. Nonetheless, it is time-consuming and costly to construct all-sided fuzzy rules; and moreover, the regulation performance relies much on practical experiences [13]. NN algorithms show strong adaptation to variation of controlling targets, and yet large amount of training job and online calculation is indispensable. Undoubtedly, it leads to a certain challenge for on-board implementation and therefore discounts feasibility of real application [14].

Currently, model predictive control (MPC) algorithms have attracted wide attention because of their capability in trajectory tracking, feedback regulation and online prediction; and consequently have been widely applied in thermal control processes [16]–[21]. Generally, MPC algorithms rely largely on accuracy of the system model, e.g., dynamic matrix control (DMC) methods [16]. When the environment changes or the constructed model does not involve all the conditions of object operation, the controlling performance of MPC algorithms usually cannot be guaranteed [17]. The generalized predictive control (GPC) algorithm, as a special case of MPC methods, incorporates multi-step prediction and receding horizon optimization of MPC algorithms and can be effectively applied to systems with large inertia and time-delay [18]. Moreover, it also enables self-tuning capability and feedback rectification, thereby easily adapting to uncertainty of environmental interference and inaccurate modeling [19]. Although GPC has been successfully verified in tracking the pre-set trajectory of controlling target, time-consuming characteristics and computational intensity cannot be tolerant due to recursive calculation of the so-called Diophantine equation and numerous matrix multiplications [20]. Instead, implicit GPC (IGPC) requires less computation intensity and retains the superior controlling performance, compared with conventional GPC. From this point of view, it may be more suitable for temperature control of industrial systems [21]. In particular, IGPC can directly identify model parameters of the system based on its inputs and outputs and does not need to solve the Diophantine equation, thereby reducing the calculation burden and improving the operating efficiency. Refs. [22], [23] detail the implementation of IGPC by introducing the open-loop prediction vectors for online identification. However, for controlling the unknown target with indeterminate parameters, the response time may increase, and the identification precision can be influenced to a large extent due to the stochastically selected initial values [23]. In [24], an implicit proportional-integral-based GPC (PIGPC) strategy is proposed to improve the controlling response by referring to the proportional-integral (PI) control; nevertheless, the poor initial response still exists and needs to be further improved.

Additionally, when the system is subject to unavoidable input constraints, the controlling algorithm usually imposes the extreme value directly to the input after it exceeds the constraint range. Nonetheless, the control quality may be deteriorated. As a consequence, optimal control algorithms have emerged to realize the optimal or suboptimal controlling performance of systems [25]. Reference [26] elaborates a body of optimization algorithms with proper consideration of constraints. As well known, predictive controller can explicitly handle the existing constraints of inputs and outputs [27]. The IGPC can optimizes the controlling inputs over a receding horizon for tracking the desired virtual control input closely while simultaneously considering multi constraints. In [28], to attain optimal control and meet requirements of constraints, the particle swarm optimization (PSO) algorithm is integrated into the receding horizon optimization of GPC. However, most of optimization algorithms usually require iterative calculation with the cost of high computation intensity [29]. In [30], the Lagrange multiplier is proposed to solve the control law of GPC with the constraints of inputs and leads to the insignificant computation labor. Moreover, to cope with coupling of multivariable systems, fusion algorithms that incorporate conventional feed-forward decoupling control and GPC have attained satisfactory control performance [31]. In addition, decoupling algorithms of predictive controllers are widely investigated, and they mainly includes two main categories: the objective function based algorithms [20], [32] and NN based methods [15], [33], both of which have been addressed to effectively overcome the nonlinear coupling influence of temperature systems.

Based on the aforementioned discussion, in this study, a systematic design of implicit PIGPC incorporating the Lagrange multiplier method is proposed for temperature control systems with varying time-delay and input constraints. The implicit PIGPC can achieve the preferable controlling performance by combining the horizontal forecast and PI feedback. To find the optimal controlling commands in the feasible sets, the Lagrange multiplier is introduced to solve the control law by transforming the nonlinear constraints into equality expressions. By this manner, the computation labor still remains almost the same, compared with the conventional IGPC algorithm. To eliminate the coupling effect of multivariable systems, an approximate decoupling method is employed by means of dispersing the objective function and taking the coupling effect as the feedforward input. Additionally, by roughly estimating the time-delay of system in advance and simplifying the inner prediction model, the computation labor of proposed algorithm can be further reduced. The simulation and experimental validation manifest that the proposed controller is more effective than the conventional IGPC introduced in [22], [23] and the classical PID controller. The main contribution of this study can be attributed to the following three aspects:

1) On the basis of IGPC, the algorithm introduces the scale factor and the integral factor, which can be adaptively regulated according to the performance index, thereby improving the controlling flexibility.
2) The algorithm deals with the input constraints of system by the Lagrange multiplier to guarantee the optimal control of temperature system. For the known

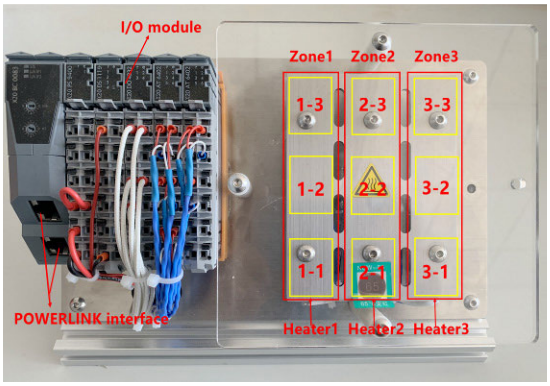

FIGURE 1. Temperature control system.

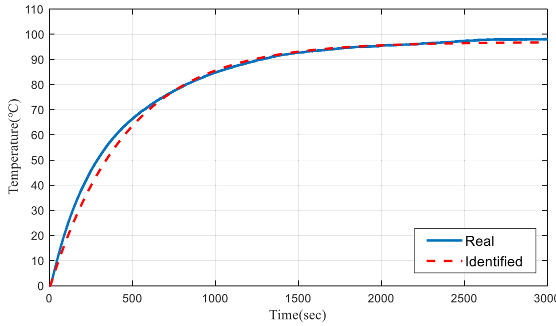

FIGURE 2. Step response curves on 2-2 temperature zone.

time-delay, the algorithm can reduce the calculation amount by simplifying the inner prediction model. Meanwhile, the extended framework of algorithm is proposed and proved effective in decoupling control of multivariable systems.

3) The algorithm overcomes the poor initial response arisen by the conventional IGPC algorithm and shows superior controlling performance including strong robustness, anti-interference and high controlling precision.

The remainder of this study is structured as follows. The modeling process of temperature control system is detailed in Section II, and Section III illustrates the design process of controller for the constrained, time-delay and coupling temperature system. Simulations are conducted to verify the feasibility of proposed controller in Section IV. Section V conducts the experiments and discusses the results on the target system to further validate the effectiveness of proposed algorithm. Section VI draws the main conclusions of this study.

II. TEMPERATURE CONTROL SYSTEM

The target temperature system, shown in Fig. 1, was developed by the B&R Industrial Automation LLC, and it is a down-scaled system to simulate a multi temperature control environment for industrial production with the characteristics of coupling, time-delay and time-variation. As can be seen, the temperatures of three zones are controlled. By controlling the duty cycle of pulse width modulation (PWM) excitation, the temperature can be regulated by three heaters. Meanwhile, three equally distributed thermocouples (zones 1-2, 2-2 and 3-2) are attached to acquire the temperature.

As introduced in previous studies [34], the temperature controlling system can be described by a first-order damp model with a certain time delay, as:

$$y = G(s) \cdot u, G(s) = \frac{K}{Ts+1} e^{-\tau} \tag{1}$$

where u denotes the duty cycle of PWM, y means the temperature of the controlled zone, K is the steady-state gain, τ represents the time delay, and T denotes the time constant. As the object is controlled only by PWM, the input constraint of system is set to $0 \leq u(t) \leq 1$. To design the controller, the model parameters should be firstly identified. In this study, the parameter identification is conducted according to the step-response inspired respectively on the three temperature zones. In this manner, the mathematical models of each temperature zone and their inter-coupling can be determined. Among them, the transfer function of zone 2-2 can be described as:

$$G_{2-2}(s) = \frac{96.94}{463.7s+1} e^{-5s} \tag{2}$$

The identification result is shown in Fig. 2, validating the effectiveness of modeling and parameter identification methods. To simplify the design of control algorithm, the following assumptions are made:

1) As shown in Fig. 2, the temperature system exhibits certain inertia, the temperature variation $f(t)$ can be approximately equal to the previous moment $y(t-1)$ when the controller period is short enough, i.e., $f(t) = y(t-1)$.
2) According to the step-response experiment, the interaction effect between zone 1 and zone 3 is small. Hence, in this study, the coupling effect between zones 1 and 3 is neglected.

In the next step, the design of controller is detailed to tackle the input constrained, time-delay and coupling problem and achieve the effective temperature control.

III. CONTROLLER DESIGN

In this paper, we focus on the temperature control of zone 2-2 and multi horizontal temperature zones (zones 1-2, 2-2, and 3-2). The target is to attain the setting temperature as soon as possible with minimization of overshoot and steady error. To this end, we designed the controller on the basis of implicit PIGPC. The structure of proposed controller is shown in Fig. 3. As can be seen, the controlling process includes five modules: 1) online identification, 2) predictive model, 3) feedback rectification, 4) constraints processing, and 5) receding horizon optimization. Firstly, an initial voltage signal is imposed to the programmable logic controller (PLC) to heat the aluminum profile, and then the

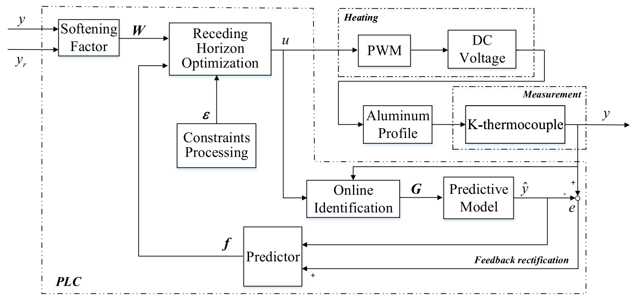

FIGURE 3. **The proposed controller structure of the target temperature system.**

temperature is monitored by the thermocouple and sent to the PLC. In the PLC, the prediction model is identified online and the feedback rectification is activated to predict the temperature. Meanwhile, the controlling input is calculated by the receding horizon optimization with the consideration of constraints. Finally, the calculated input value is fed back to the PWM module to heat the profiles.

A. IMPLICIT PIGPC

In the GPC algorithm, the prediction characteristics of single-input single-output (SISO) system can be described by the controlled auto-regressive integrated moving average (CARIMA) model, as:

$$A(z^{-1})y(t) = B(z^{-1})u(t-1) + C(z^{-1})\xi(t)/\Delta \tag{3}$$

where $A(z^{-1})$, $B(z^{-1})$ and $C(z^{-1})$ denote the polynomials of system in terms of the backward shift operator z^{-1} with the order of n_a, n_b and n_c, respectively; $y(t)$, $u(t)$ and $\xi(t)$ are the system output, input and the zero-mean random noise sequence; and $\Delta = 1 - z^{-1}$. In this study, $y(t)$ is the current temperature of system and $u(t)$ denotes the duty ratio of PWM, and obviously $0 \leq u(t) \leq 1$. To implement the proposed algorithm, the Diophantine equation is introduced, as:

$$\begin{cases} 1 = E_j(z^{-1})\Delta A(z^{-1}) + z^{-j}F_j(z^{-1}) \\ E_j(z^{-1})B(z^{-1}) = G_j(z^{-1}) + z^{-j}H_j(z^{-1}) \end{cases} \tag{4}$$

By multiplying $E_j(z^{-1})\Delta$ in (3) and simplifying (4), the output prediction value at instant $t+j$ can be calculated, as:

$$y(t+j) = G_j(z^{-1})\Delta u(t+j-1) + f(t+j) + \eta(t+j) \tag{5}$$

where $f(t+j) = F_j(z^{-1})y(t) + H_j\Delta u(t-1)$, and $\eta(t+j) = E_j(z^{-1})C(z^{-1})\xi(t+j)$. The predicted value at instant $t+j$ can be obtained by ignoring the impact of future noise, as:

$$\hat{y}(t+j/t) = G_j(z^{-1})\Delta u(t+j-1) + f(t+j) \tag{6}$$

To optimize the dynamic performance of system and prevent Δu from sudden change, we consider the variation of output temperature, deviation of temperature increment and incremental rate of inputs as the quadratic performance index by referring to the PI controller, and thus the objective function can be reformulated, as:

$$J = \sum_{j=1}^{N_1}\left[k_p\Delta e^2(t+j) + k_i e^2(t+j)\right] + \sum_{j=1}^{N_u}\lambda\left[\Delta u(t+j-1)\right]^2 \tag{7}$$

where $k_p \geq 0$ and $k_i \geq 0$ denote the given constants. k_p, as the scale factor, denotes the weighting coefficient for the error difference; and k_i, referred to as the integral factor, is the weighting coefficient of the error. N_1 denotes the length of prediction horizon, N_u is the length of control horizon, and $N_1 \geq N_u$. $\lambda > 0$ expresses the weighting coefficient of control increment. $e(t+j)$ denotes the error between the setting temperature target and actual feedback at step $t+j$, and $\Delta e(t+j)$ means the variation rate of $e(t+j)$. Thus, we can get:

$$\begin{cases} e(t+j) = w(t+j) - y(t+j) \\ \Delta e(t+j) = e(t+j) - e(t+j-1) \quad j = 1, \cdots, N_1 \end{cases} \tag{8}$$

where $w(t+j)$ denotes the reference trajectory of the temperature, and

$$w(t+j) = \alpha^j y(t) + (1-\alpha^j)y_r \quad j = 1, \cdots, N_1 \tag{9}$$

where α expresses the soften factor, $0 \leq \alpha < 1$, and y_r is the desired temperature target. By replacing $\hat{y}(t+j/t)$ in (6) with $y(t+j)$, we can attain:

$$\begin{aligned} J = {} & \Delta \boldsymbol{U}^T\left[k_p\overline{\boldsymbol{G}}^T\overline{\boldsymbol{G}} + k_i\boldsymbol{G}^T\boldsymbol{G} + \lambda\boldsymbol{I}\right]\Delta\boldsymbol{U} \\ & -2\left[k_p(\Delta\boldsymbol{W} - \Delta\boldsymbol{f})^T\overline{\boldsymbol{G}} + k_i(\boldsymbol{W} - \boldsymbol{f})^T\boldsymbol{G}\right]\Delta\boldsymbol{U} \\ & +k_p(\Delta\boldsymbol{W} - \Delta\boldsymbol{f})^T(\Delta\boldsymbol{W} - \Delta\boldsymbol{f}) \\ & +k_i(\boldsymbol{W} - \boldsymbol{f})^T(\boldsymbol{W} - \boldsymbol{f}) \end{aligned} \tag{10}$$

where, is obtained by the equation as shown at the bottom of next page.

In the case of no constraints, let $\partial J_1/\partial\Delta\boldsymbol{U} = 0$, then the optimal control law of implicit PIGPC can be determined, as:

$$\Delta\boldsymbol{U} = \boldsymbol{K}_P(\Delta\boldsymbol{W} - \Delta\boldsymbol{f}) + \boldsymbol{K}_I(\boldsymbol{W} - \boldsymbol{f}) \tag{11}$$

where $\boldsymbol{K}_P = k_p(k_p\overline{\boldsymbol{G}}^T\overline{\boldsymbol{G}} + k_i\boldsymbol{G}^T\boldsymbol{G} + \lambda\boldsymbol{I})^{-1}\overline{\boldsymbol{G}}^T$, and $\boldsymbol{K}_I = k_i(k_p\overline{\boldsymbol{G}}^T\overline{\boldsymbol{G}} + k_i\boldsymbol{G}^T\boldsymbol{G} + \lambda\boldsymbol{I})^{-1}\boldsymbol{G}^T$. To simplify the control law, we define that:

$$\boldsymbol{S} = \begin{bmatrix} 1 & & 0 \\ -1 & 1 & \\ & \ddots & \ddots \\ 0 & -1 & 1 \end{bmatrix} \tag{12}$$

Then, we can get $\overline{\boldsymbol{G}} = \boldsymbol{S}\boldsymbol{G}$, $\Delta\boldsymbol{W} = \boldsymbol{S}\boldsymbol{W}$, and $\Delta\boldsymbol{f} = \boldsymbol{S}\boldsymbol{f}$. Setting $\boldsymbol{\Omega} = \boldsymbol{K}_p\boldsymbol{S}^T\boldsymbol{S} + \boldsymbol{K}_I\boldsymbol{I}$, equation (11) can be rewritten as:

$$\Delta\boldsymbol{U} = \left(\boldsymbol{G}^T\boldsymbol{\Omega}\boldsymbol{G} + \lambda\boldsymbol{I}\right)^{-1}\boldsymbol{G}^T\boldsymbol{\Omega}(\boldsymbol{W} - \boldsymbol{f}) \tag{13}$$

Now, it can be seen from (13) that the solution matrix $\boldsymbol{G}$ and open-loop prediction vector $\boldsymbol{f}$ are required to solve for $\Delta \boldsymbol{U}$. From N_1 in (5), we can get:

$$y(t) = g_{N_1-1}\Delta u(t-N) + g_{N_1-2}\Delta u(t-N_1-1) + \cdots + g_0 \Delta u(t-1) + f(t) + \eta(t) \quad (14)$$

where $f(t)$ is the predicted free response at instant $t-1$ that cannot be affected by $\Delta u(t-1)$. In this study, we assume that $f(t) = y(t-1)$. On this basis, equation (14) can be reformulated into:

$$\Delta y(t) = g_{N_1-1}\Delta u(t-N_1) + g_{N_1-2}\Delta u(t-N_1-1) + \cdots + g_0 \Delta u(t-1) + \eta(t) \quad (15)$$

where $\boldsymbol{X}(t) = [\Delta u(t-N_1), \Delta u(t-N_1+1), \cdots \Delta u(t-1)]$, and $\boldsymbol{\theta}(t) = [g_{N_1-1}, g_{N_1-2}, \cdots g_0]^T$ can be updated by the recursive least square method with a forgetting factor, as:

$$\begin{cases} \widehat{\boldsymbol{\theta}}(t) = \widehat{\boldsymbol{\theta}}(t-1) + \boldsymbol{K}(t-1)\left(\Delta y(t) - \boldsymbol{X}(t)\widehat{\boldsymbol{\theta}}(t-1)\right) \\ \boldsymbol{K}(t) = \boldsymbol{P}(t-1)\boldsymbol{X}^T(t)\left(\lambda_1 + \boldsymbol{X}(t)\boldsymbol{P}(t-1)\boldsymbol{X}^T(t)\right)^{-1} \\ \boldsymbol{P}(t) = (\boldsymbol{I} - \boldsymbol{K}(t)\boldsymbol{X}(t))\boldsymbol{P}(t-1)\lambda_1^{-1} \end{cases} \quad (16)$$

where $\boldsymbol{K}(t)$ denotes the gain matrix of innovation; $\boldsymbol{P}(t)$ is the weighting matrix; λ_1 is the forgetting factor, $0 < \lambda_1 \le 1$; and λ_1 is set to 0.99 after trail-and-error. According to the equivalence principle of GPC and DMC [23], $\boldsymbol{f}$ represents the output of uncontrolled increment $\Delta u(t)$ for next N_1 instants at step t, and thus $\boldsymbol{f}$ in GPC equals to the initial predicted value in DMC [16], which can be expressed as:

$$\boldsymbol{f} = \begin{bmatrix} f(t+1) \\ f(t+2) \\ \vdots \\ f(t+N_1-1) \\ f(t+N_1) \end{bmatrix} = \begin{bmatrix} \hat{y}(t+1/t-1) \\ \hat{y}(t+2/t-1) \\ \vdots \\ \hat{y}(t+N_1-1/t-1) \\ \hat{y}(t+N_1-1/t-1) \end{bmatrix} + \begin{bmatrix} 1 \\ 1 \\ \vdots \\ 1 \\ 1 \end{bmatrix} e_1(t) \quad (17)$$

where $e_1(t) = y(t) - \hat{y}(t/t-1)$. After calculating $\boldsymbol{G}$ and $\boldsymbol{f}$, the control input $u(t)$ can be calculated as:

$$u(t) = u(t-1) + g^T \boldsymbol{G}^T \boldsymbol{\Omega}(\boldsymbol{W} - \boldsymbol{f}) \quad (18)$$

where $g^T = [10\cdots 0](\boldsymbol{G}^T\boldsymbol{\Omega}\boldsymbol{G} + \lambda \boldsymbol{I})^{-1}$.

Compared with the typical IGPC algorithm [22], [23], the study adopts a reasonable approximation that $f(t)$ is not involved in the identification.

B. INPUT CONSTRAINT PROCESSING

In this paper, the amplitude of control input $u(t)$ for the future j steps should be subject to:

$$u_{\min} \le u(t+j-1) \le u_{\max} \quad j = 1, \cdots, N_u \quad (19)$$

$$\begin{cases} \boldsymbol{W} = [w(t+1), w(t+2), \cdots, w(t+N_1)]^T \\ \boldsymbol{f} = [f(t+1), f(t+2), \cdots, f(t+N_1)]^T \\ \boldsymbol{G} = \begin{bmatrix} g_0 & 0 & 0 & \cdots & 0 \\ g_1 & g_0 & 0 & \cdots & 0 \\ \vdots & & & & \\ g_{N_u-1} & g_{N_u-2} & g_{N_u-3} & \cdots & g_0 \\ \vdots & & & & \\ g_{N_1-1} & g_{N_1-2} & g_{N_1-3} & \cdots & g_{N_1-N_u} \end{bmatrix} \\ \Delta\boldsymbol{W} = [\Delta w(t+1), \Delta w(t+2), \cdots, \Delta w(t+N_1)]^T \\ \Delta\boldsymbol{f} = [\Delta f(t+1), \Delta f(t+2), \cdots, \Delta f(t+N_1)]^T \\ \Delta\boldsymbol{U} = [\Delta u(t), \Delta u(t+1), \cdots, \Delta u(t+N_u-1)]^T \\ \overline{\boldsymbol{G}} = \begin{bmatrix} g_0 & 0 & \cdots & 0 \\ g_1 - g_0 & g_0 & \cdots & 0 \\ \vdots & & & \\ g_{N_u-1} - g_{N_u-2} & g_{N_u-2} - g_{N_u-3} & \cdots & g_0 \\ \vdots & & \vdots & \\ g_{N_1-1} - g_{N_1-2} & g_{N_1-2} - g_{N_1-3} & \cdots & g_{N_1-N_u} - g_{N_1-N_u-1} \end{bmatrix} \end{cases}$$

where $u(t+j-1)=u(t-1)+\sum_{i=1}^{N_u}\Delta u(t+i-1)$. By setting the upper and lower limits, we can attain:

$$u_{\min}-u(t-1)\leq\sum_{i=1}^{N_u}\Delta u(t+i-1)\leq u_{\max}-u(t-1) \quad (20)$$

Furthermore, equation (20) can be rewritten as:

$$\begin{cases} \boldsymbol{M}\Delta\boldsymbol{U}\leq\boldsymbol{U}_{\max} \\ -\boldsymbol{M}\Delta\boldsymbol{U}\leq-\boldsymbol{U}_{\min} \end{cases} \quad (21)$$

where

$$\begin{cases} \boldsymbol{U}_{\max}=[u_{\max}-u(t-1),\cdots u_{\max}-u(t-1)]^T \\ \boldsymbol{U}_{\min}=[u_{\min}-u(t-1),\cdots u_{\min}-u(t-1)]^T \\ \boldsymbol{M}=\begin{bmatrix} 1 & & & 0 \\ 1 & 1 & & \\ \vdots & \vdots & \ddots & \\ 1 & 1 & \cdots & 1 \end{bmatrix}_{N_u\times N_u} \end{cases}$$

From (21), the constraints can be summarized as:

$$\boldsymbol{A}\Delta\boldsymbol{U}\leq\boldsymbol{b} \quad (22)$$

where $\boldsymbol{A}=[\boldsymbol{M}\ -\boldsymbol{M}]^T$, and $\boldsymbol{b}=[\boldsymbol{U}_{\max}^T\ -\boldsymbol{U}_{\min}^T]^T$. Given $\boldsymbol{\Phi}=\boldsymbol{G}^T\boldsymbol{\Omega}\boldsymbol{G}+\lambda\boldsymbol{I}$, $J_0=(\boldsymbol{W}-\boldsymbol{f})^T\boldsymbol{\Omega}(\boldsymbol{W}-\boldsymbol{f})$ and $\boldsymbol{\psi}=\boldsymbol{G}^T\boldsymbol{\Omega}(\boldsymbol{W}-\boldsymbol{f})$, the optimization problem with constraints can be summarized as:

$$\begin{cases} J=\Delta\boldsymbol{U}^T\boldsymbol{\Phi}\Delta\boldsymbol{U}-2\boldsymbol{\psi}^T\Delta\boldsymbol{U}+J_0 \\ \boldsymbol{A}\Delta\boldsymbol{U}\leq\boldsymbol{b} \end{cases} \quad (23)$$

By this manner, the original problem is transformed into a quadratic optimization problem with linear inequality constraints. It can be easily proved that $\boldsymbol{\Phi}$ is the positive definite according to the definition in [35]. As such, J is a convex function, and furthermore is actually a typical convex quadratic programming problem. There exist a body of algorithms for solving the quadratic programming problem [36], most of which essentially require online iterative calculation to gradually approximate the optimal solution. Therefore, intensive computation is usually indispensable and the initial value and iterative function will also affect the convergence speed to a large extent. To accelerate the online calculation process, the Lagrange multiplier method is herein employed to cope with such constraint issue. The inequality constraint is converted into the equality constraint by adding a slack coefficient, and the analytical expression of control law is built, thereby reducing the online calculation labor and simultaneously improving the online calculation efficiency. The Lagrange function can be defined as:

$$L_x=\Delta\boldsymbol{U}^T\boldsymbol{\Phi}\Delta\boldsymbol{U}-2\boldsymbol{\psi}^T\Delta\boldsymbol{U}+J_0+\boldsymbol{\varepsilon}^T(\boldsymbol{A}\Delta\boldsymbol{U}-\boldsymbol{b}) \quad (24)$$

where $\boldsymbol{\varepsilon}$ denotes the Lagrange multiplier matrix, and $\boldsymbol{\varepsilon}=\left[\varepsilon_1^*\cdots\varepsilon_{2\times N_u}^*\right]$. The inequality constraint problem can be solved only if the Karush-Kuhn-Tucker (KKT) condition is satisfied [37], as:

$$\begin{cases} \nabla_{\Delta u}L(\Delta u,\boldsymbol{\varepsilon}^*)=0 \\ \boldsymbol{\varepsilon}^*\geq 0 \\ \boldsymbol{\varepsilon}^*(\boldsymbol{A}\Delta u-\boldsymbol{b})=0 \end{cases} \quad (25)$$

On this account, by solving the partial derivative of (24) with respect to $\Delta\boldsymbol{U}$ and $\boldsymbol{\varepsilon}$, as:

$$\begin{cases} \dfrac{\partial L_x}{\partial\Delta\boldsymbol{U}}=(\boldsymbol{\Phi}^T+\boldsymbol{\Phi})\Delta\boldsymbol{U}-2\boldsymbol{\psi}+\boldsymbol{A}^T\boldsymbol{\varepsilon}=0 \\ \dfrac{\partial L_x}{\partial\boldsymbol{\varepsilon}}=\boldsymbol{A}\Delta\boldsymbol{U}-\boldsymbol{b}=0 \end{cases} \quad (26)$$

we can attain:

$$\begin{cases} \Delta\boldsymbol{U}=\boldsymbol{\Phi}^{-1}(\boldsymbol{\psi}-\dfrac{1}{2}\boldsymbol{A}^T\boldsymbol{\varepsilon}) \\ \boldsymbol{\varepsilon}=\dfrac{2(\boldsymbol{A}\boldsymbol{\Phi}^{-1}\boldsymbol{\psi}-\boldsymbol{b})}{\boldsymbol{A}\boldsymbol{\Phi}^{-1}\boldsymbol{A}^T} \end{cases} \quad (27)$$

Based on (27), $\boldsymbol{\varepsilon}$ can be solved to determine whether the constraint takes effect in the solution value. $\varepsilon^*<0$ indicates that the inequality constraint does not work for $\Delta\boldsymbol{U}$, then the constraint inequality needs to be canceled, and $\varepsilon^*=0$. In contrast, $\varepsilon^*>0$ suggests that the inequality is the constraint imposed on $\Delta\boldsymbol{U}$ and ε^* is retained to satisfy the KKT condition. Now, according to (13), the control law can be finally attained:

$$\Delta\boldsymbol{U}=(\boldsymbol{G}^T\boldsymbol{\Omega}\boldsymbol{G}+\lambda\boldsymbol{I})^{-1}\left[\boldsymbol{G}^T\boldsymbol{\Omega}(\boldsymbol{W}-\boldsymbol{f})-\frac{1}{2}\boldsymbol{A}^T\boldsymbol{\varepsilon}\right] \quad (28)$$

C. TIME DELAY

When the predictive control algorithm is applied to the pure time-delay object, the time lag can be directly considered within the algorithm, which is equivalent by adding an output delay to the non-lag part. As such, for the system with known time-delay τ, the proposed controller can be simplified by the following calculation:

$$l=\tau/T_0,\quad l\in Z \quad (29)$$

where T_0 denotes the control cycle, and l is the lag steps of system. Since the system has no output in the delay process, the control law coefficient of the first l steps of system can be regarded as 0. Therefore, the optimized domain on the identification process can be taken as $N_0=N_1-l$, and the matrix $\boldsymbol{G}$ can be calculated, as:

$$\hat{\boldsymbol{G}}=\left[\boldsymbol{0}_{l\times N_u};\boldsymbol{G}_{N_0\times N_u}\right] \quad (30)$$

In summary, the controller can save the calculation labor in a large time-delay system and becomes feasible to implement in real application.

D. MULTIVARIABLE CONTROLLER EXTENSION

With regard to multi-input multi-output (MIMO) systems, decentralization of the objective function should be conducted, and the coupling problem is usually solved by the

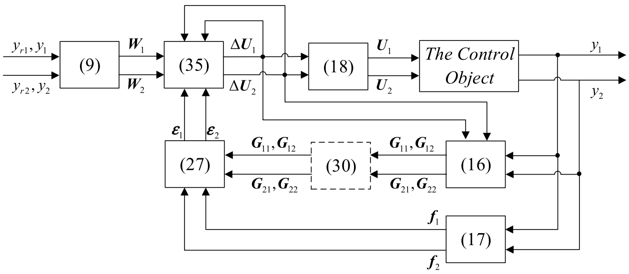

FIGURE 4. The controller structure.

feedforward decoupling strategy. By this way, the multivariable controller can be transferred into a SISO controller optimization problem. Supposing the multivariable system has p inputs and q outputs, its performance metrics can be divided into the performance indexes for q subsystems, as:

$$J_M = J_1 + J_2 + \cdots + J_q \tag{31}$$

where J_q is the objective functions of subsystem q, and

$$J_q = \sum_{j=1}^{N_1}\left[k_p \Delta e_q^2(t+j) + k_i e_q^2(t+j)\right] + \sum_{j=1}^{N_u} \lambda \left[\Delta u_q(t+j-1)\right]^2 \tag{32}$$

According to (6), the predicted output of subsystem q can be expressed as:

$$\hat{\boldsymbol{Y}}_q = \boldsymbol{G}_{q1}\Delta\boldsymbol{U}_1 + \cdots + \boldsymbol{G}_{qp}\Delta\boldsymbol{U}_p + \boldsymbol{G}_{qx}\Delta\boldsymbol{U}_x + \boldsymbol{f}_q \tag{33}$$

where $\boldsymbol{G}_{qx}$ and $\Delta\boldsymbol{U}_x$ denote the coefficient matrix and control increment matrix of the direct action on subsystem q. $\boldsymbol{G}_{q1}, \cdots, \boldsymbol{G}_{qp}$ denote the coupling coefficients of subsystems 1 to p in terms of subsystem q, which can be identified by (16). In this paper, $\Delta\boldsymbol{U}_1 \cdots \Delta\boldsymbol{U}_p$ at t is replaced by $\Delta\boldsymbol{U}_1 \cdots \Delta\boldsymbol{U}_p$ at $t-1$, and therefore $\boldsymbol{G}_{q1}\Delta\boldsymbol{U}_1 \cdots \boldsymbol{G}_{qp}\Delta\boldsymbol{U}_p$ can be regarded as the known values, which is substituted into the system for the feedforward decoupling control. Thus, equation (33) can be transferred into:

$$\begin{cases} \hat{\boldsymbol{Y}}_q = \boldsymbol{G}_{qx}\Delta\boldsymbol{U}_x + \bar{\boldsymbol{f}}_q \\ \bar{\boldsymbol{f}}_q = \boldsymbol{G}_{q1}\Delta\boldsymbol{U}_1 + \cdots + \boldsymbol{G}_{qp}\Delta\boldsymbol{U}_p + \boldsymbol{f}_q \end{cases} \tag{34}$$

Based on (28), the control law can be derived, as:

$$\Delta\boldsymbol{U}_q = \boldsymbol{\Phi}_q^{-1}\left(\boldsymbol{G}_{qx}^T\boldsymbol{\Omega}(\boldsymbol{W}_q - \bar{\boldsymbol{f}}_q) - \frac{1}{2}\boldsymbol{A}^T\boldsymbol{\varepsilon}_q\right) \tag{35}$$

where $\boldsymbol{\Phi}_q = \boldsymbol{G}_{qx}^T\boldsymbol{\Omega}\boldsymbol{G}_{qx} + \lambda\boldsymbol{I}$. According to (34), the multivariable controller only considers the coupling effect $\boldsymbol{G}_{q1}\Delta\boldsymbol{U}_1 \cdots \boldsymbol{G}_{qp}\Delta\boldsymbol{U}_p$ as the known value, which is treated as the new free response $\bar{\boldsymbol{f}}_q$ on the basis of the univariate controller. Therefore, the multivariate form is an extension of single univariate controller, and shows certain universality. The controller structure ($p = q = 2$) is shown in Fig. 4.

In summary, the implementation process of proposed controller for the SISO or MIMO system is described as follows:

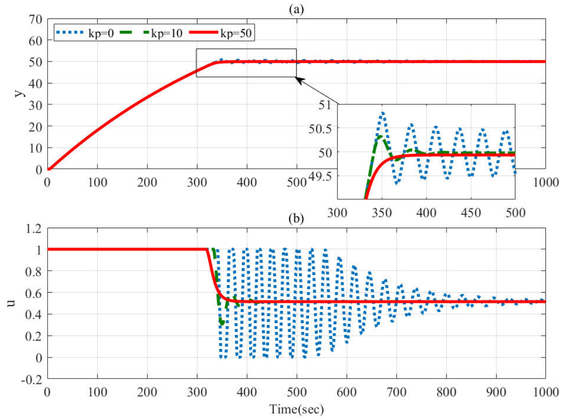

FIGURE 5. Influence of scale factor k_p on the stability of controller. (a) The response; (b) The control quantity.

Step 1: Assign the initial values to N_1, N_0, N_u, λ, α, k_p and k_i;

Step 2: Apply (16) to identify the parameter matrix $\boldsymbol{G}(\boldsymbol{G}_{11} \cdots \boldsymbol{G}_{pp})$, and calculate (17) to get the prediction vector $\boldsymbol{f}(\boldsymbol{f}_1 \cdots \boldsymbol{f}_p)$;

Step 3: Calculate $\boldsymbol{\varepsilon}$ according to (27). If $\varepsilon^* < 0$, set $\varepsilon^* = 0$; otherwise keep it;

Step 4: Calculate the system control laws based on (28) or (35) according to the amount of controlling variables;

Step 5: Repeat steps 2 to 4 until the end.

In the next step, numerical simulations are conducted to validate the proposed controller.

IV. NUMERICAL SIMULATION

To validate the parameter setting principle of controller and justify the feasibility of proposed controller, numerical simulations were conducted in Matlab/Simulink, and the detailed numerical analysis are performed.

A. PARAMETER TUNNING PRINCIPLE

The selection of controller parameters can directly affect the controlling performance. Compared with the conventional IGPC, the proposed algorithm adds two extra variables, k_p and k_i. Firstly, the function of k_p and k_i is discussed through simulation, and the other parameters can be referred in [21]. In this study, we select the zone 2-2 as the simulation object, and its mathematical model G_{2-2} is shown in (2). The following parameters are set as: $N_1 = 15$, $N_0 = 10$, $N_u = 2$, $\lambda = 0.1$ and $\alpha = 0.5$. The control period is set to 1 s. Firstly, the influence of scale factor k_p on controller is addressed, including k_p equals 0, 10 and 50, respectively. In this case, k_i equals one. The simulation results are shown in Fig. 5. As can be observed, when k_p increases, the temperature response changes more smoothly, the corresponding output becomes more stable, and meanwhile the overshoot declines. It is worth noting that the algorithm becomes the IGPC when $k_p = 0$. In summary, compared with the IGPC, k_p in the proposed algorithm can effectively improve the overall controlling performance. Larger k_p enables the system

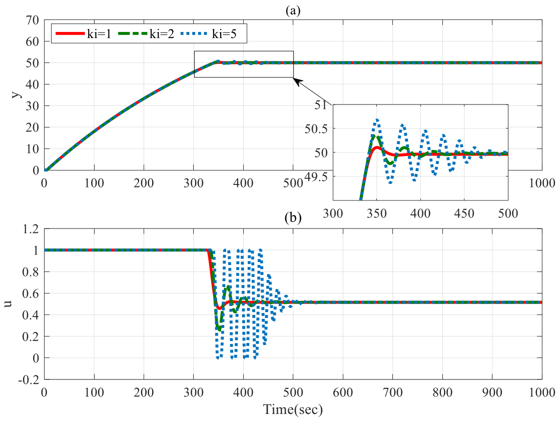

FIGURE 6. Influence of integrating factor k_i on the stability of controller. (a) The response; (b) The control quantity.

TABLE 1. Controlling parameters.

Parameters	N_1	N_0	N_u	λ	α	k_p	k_i
Proposed	15	10	2	0.1	0.9	20	1
Conventional IGPC	16	-	2	0.1	0.9	-	-

to reach the desired value faster when the variation rate of deviation is smaller. Thus, the larger k_p, the smoother the control input will be, and the better the stability will be attained. When comparing the controlling performance with different k_i, we set that $k_p = 20$ and k_i equals 1, 2 and 5, respectively. The corresponding results are shown in Fig. 6. It can be found that when k_i increases, the control output changes more obviously, the overshoot increases slightly, and the stability becomes worse than before. As k_i is the weighting coefficient of the error term, larger k_i facilitates the system to reduce the difference between the set value faster. Certainly, faster dynamic response may worsen the stability. To sum up, k_p and k_i need to be well tuned according to the control target requirements, making the controller more flexible in engineering practice.

B. SIMULATION RESULT

Simulations in terms of single temperature zone and multi-temperature zones are respectively conducted to verify the effectiveness of proposed controller. Firstly, the single temperature zone G_{2-2} is simulated. The temperature is set to change from 30 °C to 80 °C, and the simulation result is shown in Fig. 7, in which the controller parameters after tuning are shown in Table 1 and the control interval of simulation is 1 s. It can be observed that the proposed algorithm can track the setting value with quite small overshoot and almost zero steady state error. Meanwhile, the control variation is kept within the range of given constraints, verifying the effectiveness of the proposed controller.

The conventional IGPC with mandatory constraints, detailed in [22], [23], is adopted in the zone 2-2 and the controlling performance is compared with that of the

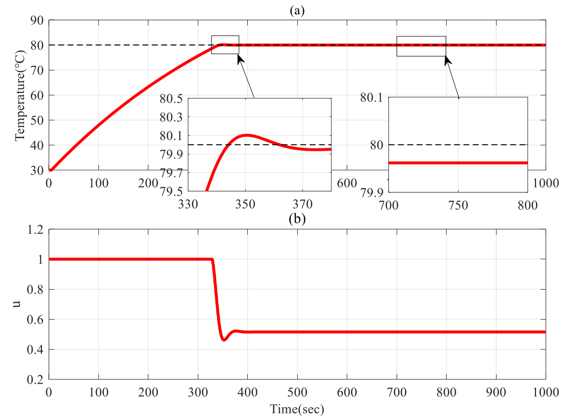

FIGURE 7. Simulation results of the 2-2 temperature zone by using the proposed controller. (a) The response; (b) The control quantity.

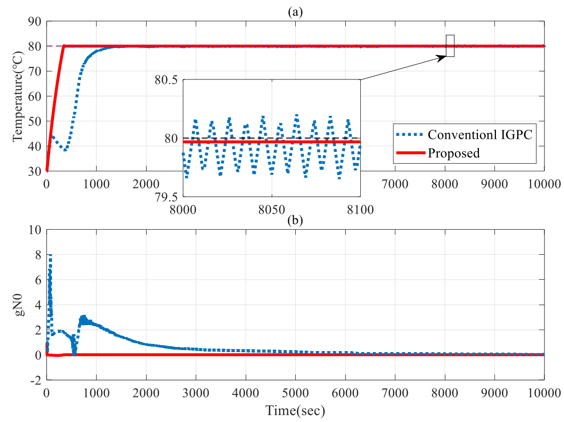

FIGURE 8. Simulation results of the 2-2 temperature zone by using the proposed method and conventional IGPC. (a) The response; (b) The identification result of the parameter.

proposed algorithm. The result is shown in Fig. 8, where Fig. 8 (a) denotes the output response and Fig. 8 (b) expresses the identification result of g_{N_0}. From Fig. 8 (b), the identified parameters of conventional IGPC converge much slower than those of the proposed algorithm. Compared with the conventional IGPC, the proposed algorithm enables faster identification. Therefore, the proposed controller can effectively overcome the influences of poor initial response of conventional IGPC.

To demonstrate the rationality of assumption 1), i.e. $f(t) \doteq y(t-1)$, the zone 2-2 is firstly heated for 100 s, and then the system input is set to 0. After that, the output of system turns to free response. The errors among $\hat{f}(t)$ obtained by the conventional IGPC, $y(t-1)$ provided by the proposed controller, and the actual $f(t)$ are compared. Fig. 9 (a) describes the curves of two processing methods, and Fig. 9 (b) compares the errors. It can be observed that the difference between $y(t-1)$ regulated by the proposed method and the actual $f(t)$ is less than 0.17, which can be almost ignored. In contrast, inaccurate $\hat{f}(t)$ of the conventional IGPC leads to unstable dynamic response to some extent. In summary, the proposed method can supply more accurate identification results, proving reasonable identification precision.

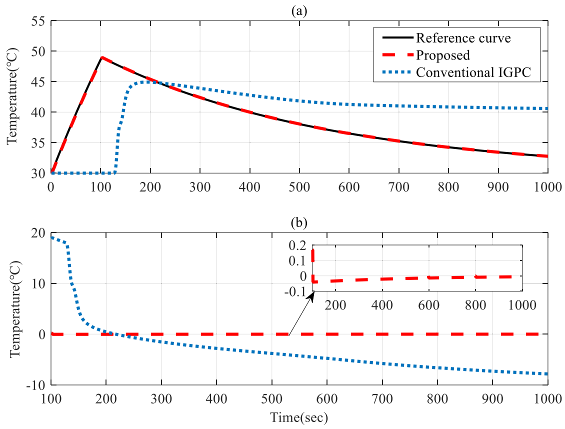

FIGURE 9. Free response $f(t)$ comparison of the proposed method and conventional IGPC. (a) The response; (b) The error.

In addition, according to Fig. 4 in Section III, the simulation is performed to further verify the performance of proposed multivariable controller. According to the assumption 2), the intermediate horizontal temperature zones (1-2, 2-2 and 3-2) are selected as the controlling target, and the mathematical model is:

$$G_2(s) = \begin{bmatrix} G_{12} \\ G_{22} \\ G_{32} \end{bmatrix} = \begin{bmatrix} \frac{116.33}{458.1s+1}e^{-6s} & \frac{61.71}{822.24s+1}e^{-65s} & 0 \\ \frac{87.83}{947.58s+1}e^{-15s} & \frac{96.94}{463.7s+1}e^{-5s} & \frac{43.7}{463.7s+1}e^{-55s} \\ 0 & \frac{46.74}{719.01s+1}e^{-86s} & \frac{106.49}{447.27s+1}e^{-6s} \end{bmatrix} \tag{36}$$

The three temperature zones are regulated from 30 °C to 100 °C simultaneously and the predictive horizon N_1 is set to 8, and the remaining parameters are kept the same as those listed in Table 1. The simulation results shown in Fig. 10 highlight that the overshoot of each temperature zone is less than 2 °C and the stability error is within 0.4 °C. From an overall perspective, the proposed controller shows preferable controlling performance and therefore the feasibility of designed multivariable decoupling controller is verified.

C. COMPARISON OF THE SIMULATION TIME

The proposed controller can reduce the computation with known time-delay. Based on the simulation results in terms of the zone 2-2, the simulation time of conventional IGPC and proposed controller with unknown time-delay ($N_0 = N_1$) and the proposed controller with known delay ($N_0 = N_1 - l$) is compared in Table 2. It can be found that the proposed method incurs least computation intensity, compared with the method of unknown time-delay ($N_0 = N_1$) with the same hardware setup. Meanwhile, compared with the conventional IGPC, the proposed method does not increase the computation intensity obviously, but leads to much better control performance. If the system has large time-delay, it can save more computation time and thus be easier to implement in engineering practice.

To sum up, the simulation results fully demonstrate the feasibility of designed controller. In the next step, the experimental validation is conducted to further verify the proposed algorithm.

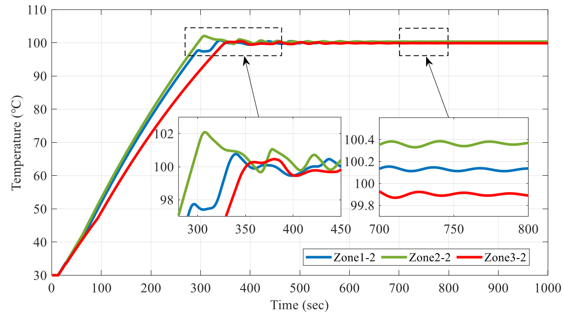

FIGURE 10. Simulation results by using the multivariate proposed controller.

TABLE 2. Simulation time.

Random Experiment	1 (s)	2 (s)	3 (s)	Average Time (s)
Conventional IGPC	2.300	2.256	2.289	2.282
Proposed ($N_0 = N_1$)	2.269	2.358	2.435	2.354
Proposed ($N_0 = N_1 - l$)	2.301	2.274	2.336	2.304

V. EXPERIMENT RESULTS AND DISCUSSION

The proposed controller, the classic PID controller and the conventional GPC controller detailed in [18] are respectively applied to the real system to verify and evaluate the performance. It is necessary to note that the inputs of GPC and PID controller adopt the mandatory constraint between 0 and 1. The built platform is shown in Fig. 11. To comprehensively evaluate the controlling performance, the following four experiments are conducted. The control goal of these experiments is to attain the setting value as rapidly as possible while trying to avoid overshoot and keep the least steady state error.

Case 1: Validate the control performance of three controllers and control the zone 2-2 from 30 °C to 80 °C. The related parameters of proposed controller are the same as those for simulation. The well-tuned parameters of classic PID controller and GPC controller are shown in Tables 3 and 4, respectively.

Case 2: Test the robustness of three controllers and change the control target for the zone 2-3 with the same parameters on the basis of Case 1. The mathematical model of the zone

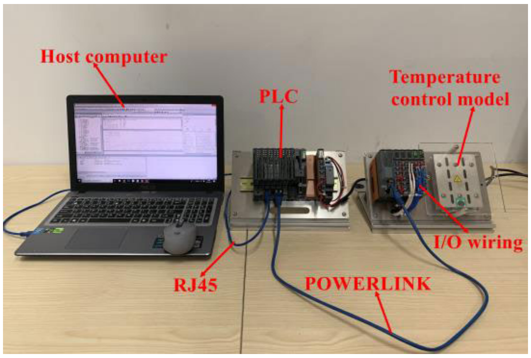

FIGURE 11. The experimental platform of temperature control system.

TABLE 3. Control parameters of PID.

Parameters	Control cycle	k_P	k_I	k_D
Case1	0.01s	1.2	50	1
Case4	0.01s	0.8	20	1

TABLE 4. Control parameters of GPC.

Parameters	Control cycle	N_1	N_u	λ	α
Case1	5 s	20	5	0.1	0.9
Case4	5 s	12	8	0.5	0.5

2-3 can be described as:

$$G_{2-3}(s) = \frac{88.33}{487.1s+1}e^{-12s} \tag{37}$$

Case 3: Verify the anti-interference of three controllers and regulate the zone 2-2 to 90 °C with the same controlling parameters as those in Case 1; and after entering the steady state, turn on the cooling fan for 100 s.

Case 4: Validate the control performance of three controllers and adjust the intermediate horizontal temperature zone from 30 °C to 100 °C simultaneously. The multivariable PID controller and GPC controller are realized by parallel connection of three univariate controllers with the same parameters. The parameters of multivariable controller are the same with those for simulation. The parameters of the multivariable PID controller and GPC controller are shown in Tables 3 and 4, respectively.

The experimental results with the sampling period of 1 s are shown in Figs. 12 to 15 and the intuitively quantified results are illustrated in Tables 5 to 8, respectively. Figs. 12 to 14 depict the experimental results of the single temperature zone for Cases 1 to 3, where (a) shows the response of three controllers, (b) presents the control quantity of three controllers. Fig. 15 depicts the results of multi-temperature zone experiment of Case 4, where (a) shows the response of PID controller, (b) presents the response of GPC controller and (c) depicts the response of proposed controller. In this study, the mean tracking error (MTE) is introduced to evaluate the tracking performance of controller, as:

$$MTE = \frac{1}{n}\sum_{i=1}^{n}|y(t) - y_r| \tag{38}$$

where n is the number of samples, $y(t)$ is the output value of the samples, and y_r is the referred value

From Fig. 12 (a), it can be observed that all the three algorithms can effectively control the temperature of zone 2-2, and the rising time of three methods is mostly the same; however the controlling performance of proposed controller

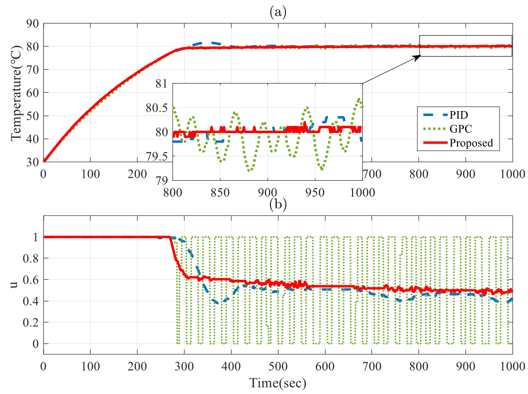

FIGURE 12. Experiment results of case 1. (a) The response; and (b) The control quantity.

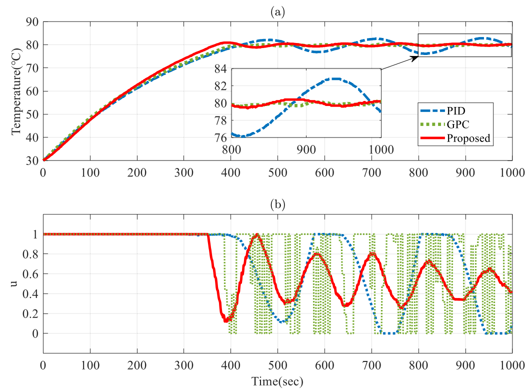

FIGURE 13. Experiment results of case 2. (a) The response; (b) The control quantity.

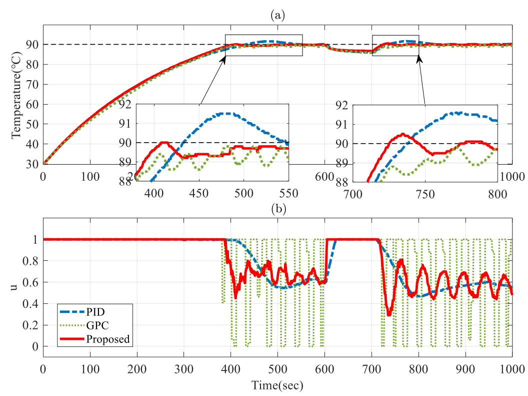

FIGURE 14. Experiment results of case 3. (a) The response; (b) The control quantity.

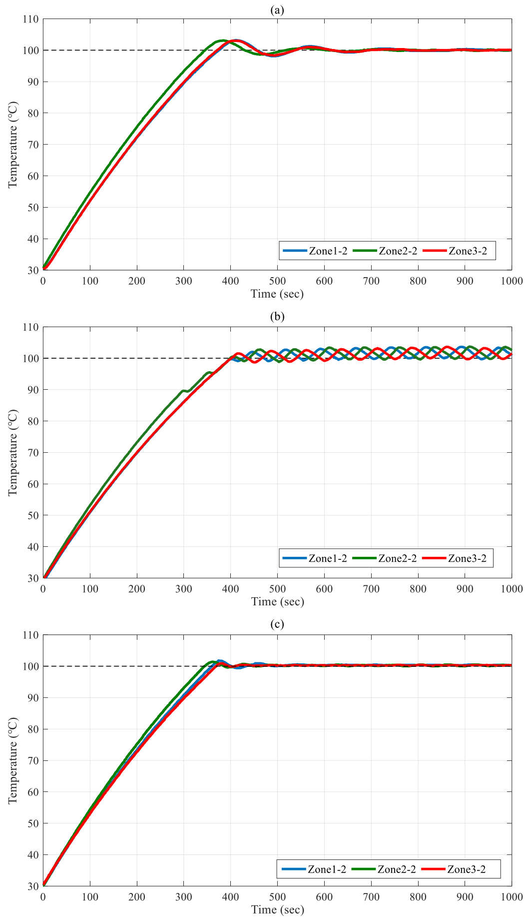

FIGURE 15. Experiment results of case 4. (a) The response of the PID controller; (b) The response of the GPC controller; (c) The response of the proposed controller.

TABLE 5. Experiment results of Case 1.

Control Method	Overshoot	MTE
PID	2.26%	6.413
GPC	0	6.606
Proposed	0	6.400

TABLE 6. Experiment results of Case 2.

Control Method	Overshoot	MTE
PID	4.06%	9.517
GPC	0.13%	7.471
Proposed	0.25%	8.231

is obviously superior to those of the other two controllers. As can be found in Fig. 12 (b), the controlling input profile based on the proposed controller is smoother, and its steady-state error is less than that of PID and GPC, only within 0.1 °C. As listed in Table 5, the results of proposed algorithm show no overshoot and the MTE of proposed controller are less than those of the other controllers. It is worth pointing out that the GPC algorithm introduced in [18] needs to know the system model parameters in advance, and the

TABLE 7. Experiment results of Case 3.

Control Method	Overshoot (700s)	MTE (700 s-1000 s)
PID	1.78%	0.629
GPC	0	0.963
Proposed	0.56%	0.326

TABLE 8. Experiment results of Case 4.

Control Method	Performance index	Zone 1-2	Zone 2-2	Zone 3-2	Average value
PID	Overshoot	3.2%,	3.1%	2.9%	3.07%
	MTE	12.41	11.20	12.29	11.97
GPC	Overshoot	2%	0.6%	1.5%	1.37%
	MTE	13.6610	12.7783	13.5229	13.321
Proposed	Overshoot	1.5%	1.2%	0.6%	1.1%
	MTE	11.7968	11.1884	11.8904	11.625

predicted output may deviate from the actual output when the model is inaccurate or the parameters change. In this case, the calculated control quantity does not meet the system requirements and thus degrades the final controlling performance. In contrast, the proposed algorithm can dynamically adapt to the environmental variation, directly obtain the control quantity only by the input and output data of the system and still gain superior control performance. Meanwhile, compared with the conventional GPC algorithm, the additive PI controlling topology and proper treatment of constraints enables the better responses in terms of overshoot and steady error. In Fig. 13 (a), it is obvious that the proposed algorithm can still achieve the anticipated performance when the model changes, and the PID controller incurs more overshoot and oscillation, and the response curve changes more sharply, and the regulation target is not attained. According to Table 6, the overshoot of proposed algorithm is 0.25%, which is 3.81% less than that of the PID controller and the MTE of proposed algorithm is 1.286, much less than that of PID controller.

As shown in Fig. 14 (a), the heating-up response with less overshoot is achieved by the proposed method, compared with the PID controller when the target temperature is 90 °C and the steady state error of proposed method is less than that of the GPC algorithm. Additionally, when the disturbance is invaded, the proposed controller can adjust the controlling input more quickly and features stronger adaptability and better anti-disturbance performance, when comparing with other two controllers, due to the capability of online identification and feedback automatic correction. The performance metrics after 700 s are listed in Table 7, and the MTE of proposed controller is the smallest. It is obviously found from Fig. 15 that the overshoot of PID algorithm is quite large and the steady-state error of GPC algorithm cannot be tolerant. From a comprehensive perspective, the proposed algorithm is capable of controlling multiple temperature zones in a more efficient and effective manner. The data in Table 8 shows that the average overshoot of three temperature zones of proposed controller is 1.1%, which is much less than those of the other two controllers, and the average MTE of three temperature zones is 11.625, verifying the feasibility of proposed PIGPC controller.

VI. CONCLUSION

This paper designed an implicit PIGPC controller for temperature control systems. The proposed controller adopts the recursive least square method with the forgetting factor to identify the parameters of control law online, which can correct the mismatched model in time and improve the model stability. Meanwhile, the proposed algorithm enables faster identification convergence and overcomes the poor initial response arisen by the conventional IGPC algorithm. The proposed controller introduces the scale factor and the integrating factor based on the IGPC algorithm, making the controller more flexible and leading to better controlling performance. The Lagrange multiplier method, which requires less computation, is introduced to enable the controller easier to solve the optimal problem when subject to constraints. For system with known time delay, a simplified internal prediction model is proposed to reduce the computational intensity of the algorithm. Additionally, a multivariable extension framework of the proposed algorithm is designed, and the effectiveness of proposed decoupling control for multivariable system is validated. The simulation and experiments results manifest the effectiveness of the proposed controller, which exhibits superior controlling performance including strong robustness, anti-interference and high precision, compared with conventional GPC algorithm and PID controller.

ACKNOWLEDGMENT

The authors would like to thank the B&R Industrial Automation LLC for their hardware and program training support. Moreover and most importantly. They would also like to thank the anonymous reviewers for their helpful comments and suggestions.

REFERENCES

[1] G. Yuan, J. Du, and T. Yu, "Performance assessment of power plant main steam temperature control system based on ADRC control," *Int. J. Control Automat.*, vol. 8, no. 1, pp. 305–316, Jan. 2015.

[2] S. C. Rowe, I. Hischier, A. W. Palumbo, B. A. Chubukov, M. A. Wallace, R. Viger, A. Lewandowski, D. E. Clough, and A. W. Weimer, "Nowcasting, predictive control, and feedback control for temperature regulation in a novel hybrid solar-electric reactor for continuous solar-thermal chemical processing," *Solar Energy*, vol. 174, pp. 474–488, Nov. 2018.

[3] W. Xu, J. Zhang, and R. Zhang, "Application of multi-model switching predictive functional control on the temperature system of an electric heating furnace," *ISA Trans.*, vol. 68, pp. 287–292, May 2017.

[4] T. Liu, K. Yao, and F. Gao, "Identification and autotuning of temperature-control system with application to injection molding," *IEEE Trans. Control Syst. Technol.*, vol. 17, no. 6, pp. 1282–1294, Nov. 2009.

[5] J. S.-H. Tsai, F. Ebrahimzadeh, W.-T. Hsu, J. W. Tann, S.-M. Guo, L.-S. Shieh, J. I. Canelon, and L. Wang, "Modeling and tracker for unknown nonlinear stochastic delay systems with positive input constraints," *Appl. Math. Model.*, vol. 40, nos. 23–24, pp. 10447–10479, Dec. 2016.

[6] W.-J. He, H.-T. Zhang, Z. Chen, B. Chu, K. Cao, B. Shan, and R. Chen, "Generalized predictive control of temperature on an atomic layer deposition reactor," *IEEE Trans. Control Syst. Technol.*, vol. 23, no. 6, pp. 2408–2415, Nov. 2015.

[7] C. Vermillion, J. Sun, and K. Butts, "Predictive control allocation for a thermal management system based on an inner loop reference model-design, analysis, and experimental results," *IEEE Trans. Control Syst. Technol.*, vol. 19, no. 4, pp. 772–781, Jul. 2011.

[8] C. J. Chen, K. T. Wu, and S. J. M. Hwang, "Development of a servo-hydraulic system with a self-tuning fuzzy PID controller to simulate injection molding process," *Microsyst. Technol.*, no. 10, pp. 1–22, 2018, doi: 10.1007/s00542-018-4171-0.

[9] K. Tan, S. Zhao, and J.-X. Xu, "Online automatic tuning of a proportional integral derivative controller based on an iterative learning control approach," *IET Control Theory Appl.*, vol. 1, no. 1, pp. 90–96, Jan. 2007.

[10] N. S. Özbek and İ. Eker, "Design of an optimal fractional fuzzy gain-scheduled smith predictor for a time-delay process with experimental application," *ISA Trans.*, to be published.

[11] S. A. C. Giraldo, R. C. C. Flesch, and J. E. Normey-Rico, "Multivariable greenhouse control using the filtered smith predictor," *J. Control Autom. Electr. Syst.*, vol. 27, no. 4, pp. 349–358, Aug. 2016.

[12] S. F. Dos Santos Vidal, J. E. Schmitz, I. C. Franco, A. M. F. Fileti, and F. V. Da Silva, "Fuzzy multivariable control strategy applied to a refrigeration system," *Chem. Product Process Model.*, vol. 12, no. 2, pp. 1–8, 2017.

[13] H. Huang, S. Zhang, Z. Yang, Y. Tian, X. Zhao, Z. Yuan, S. Hao, J. Leng, and Y. Wei, "Modified smith fuzzy PID temperature control in an oil-replenishing device for deep-sea hydraulic system," *Ocean Eng.*, vol. 149, pp. 14–22, Feb. 2018.

[14] K. Katić, R. Li, J. Verhaart, and W. Zeiler, "Neural network based predictive control of personalized heating systems," *Energy Buildings*, vol. 174, pp. 199–213, Sep. 2018.

[15] F. Pazhooh, F. Shahraki, J. Sadeghi, and M. Fakhroleslam, "Multivariable adaptive neural network predictive control in the presence of measurement time-delay; application in control of Vinyl Acetate monomer process," *J. Process Control*, vol. 66, pp. 39–50, Jun. 2018.

[16] D. M. Lima, J. E. Normey-Rico, and T. L. M. Santos, "Temperature control in a solar collector field using filtered dynamic matrix control," *ISA Trans.*, vol. 62, pp. 39–49, May 2016.

[17] B. S. Taysom, C. D. Sorensen, and J. D. Hedengren, "A comparison of model predictive control and PID temperature control in friction stir welding," *J. Manuf. Process.*, vol. 29, pp. 232–241, Oct. 2017.

[18] A. Ramdani and S. Grouni, "Dynamic matrix control and generalized predictive control, comparison study with IMC-PID," *Int. J. Hydrogen Energy*, vol. 42, no. 28, pp. 17561–17570, Jul. 2017.

[19] Z. Li and G. Wang, "Generalized predictive control of linear time-varying systems," *J. Franklin Inst.*, vol. 354, no. 4, pp. 1819–1832, Mar. 2017.

[20] J. Zhang, Y. Zhou, Y. Li, G. Hou, and F. Fang, "Generalized predictive control applied in waste heat recovery power plants," *Appl. Energy*, vol. 102, pp. 320–326, Feb. 2013.

[21] B. Xiao, X. Zhang, and X. Dong, "Superheated steam temperature control research of the improved implicit generalized predictive algorithm based on the soft coefficient matrix," *J. Comput. Theor. Nanosci.*, vol. 9, no. 10, pp. 1733–1740, Oct. 2012.

[22] X. Lu, B. Ma, and H. Dong, "Optimization control of ATO-S based on implicit generalized predictive of chaotic particle swarm algorithm," *Int. J. Control Autom.*, vol. 8, no. 5, pp. 199–208, 2015.

[23] K. Peng, D. Fan, F. Yang, Q. Fu, and Y. Li, "Active generalized predictive control of turbine tip clearance for aero-engines," *Chin. J. Aeronaut.*, vol. 26, no. 5, pp. 1147–1155, Oct. 2013.

[24] Z.-D. Tian, X.-W. Gao, B.-L. Gong, and T. Shi, "Time-delay compensation method for networked control system based on time-delay prediction and implicit PIGPC," *Int. J. Autom. Comput.*, vol. 12, no. 6, pp. 648–656, Dec. 2015.

[25] B. Grandvallet, A. Zemouche, H. Souley-Ali, and M. Boutayeb, "New LMI condition for observer-based $\mathcal{H}_\infty$ stabilization of a class of nonlinear discrete-time systems," *SIAM J. Control Optim.*, vol. 51, no. 1, pp. 784–800, Jan. 2013.

[26] S. Vrkalovic, E.-C. Lunca, and I.-D. Borlea, "Model-free sliding mode and fuzzy controllers for reverse osmosis desalination plants," *Int. J. Artif. Intell.*, vol. 16, no. 2, pp. 208–222, 2018.

[27] J. M. Maciejowski, P. J. Goulart, and E. C. Kerrigan, *Constrained Control Using Model Predictive Control* (Lecture Notes in Control and Information Sciences), vol. 346. Berlin, Germany: Springer, 2007.

[28] J. Smoczek and J. Szpytko, "Particle swarm optimization-based multivariable generalized predictive control for an overhead crane," *IEEE/ASME Trans. Mechatronics*, vol. 22, no. 1, pp. 258–268, Feb. 2017.

[29] S. Preitl, R.-E. Precup, Z. Preitl, S. Vaivoda, S. Kilyeni, and J. K. Tar, ''Iterative feedback and learning control. Servo systems applications,'' *IFAC Proc. Volumes*, vol. vol., 40, no. 8, pp. 16–27, 2007.

[30] T. Tsang and D. W. Clarke, ''Generalised predictive control with input constraints,'' *IEE Proc. D, Control Theory Appl.*, vol. 135, no. 6, pp. 451–460, 1988.

[31] T. Chai, X. Qin, and K. Mao, ''Decoupling design of multivariable generalised predictive control,'' *IEE Proc.-Control Theory Appl.*, vol. 141, no. 3, pp. 197–201, May 1994.

[32] R. Zhang and F. Gao, ''An improved decoupling structure based state space MPC design with improved performance,'' *Syst. Control Lett.*, vol. 75, pp. 77–83, Jan. 2015.

[33] Y. Peng, L. Li, P. Liu, and Z. Yan, ''Multivariable neural network predictive control based on variable structure objective optimization,'' in *Proc. Control Decis. Conf.*, Jun. 2008.

[34] M. F. Modest, *Radiative Heat Transfer*, 2nd ed. Amsterdam, The Netherlands: Elsevier, 2003, pp. 1–822.

[35] C. R. Johnson, ''Positive definite matrices,'' *Amer. Math. Monthly*, vol. 77, no. 3, pp. 259–264, 1970.

[36] G. Cimini and A. Bemporad, ''Complexity and convergence certification of a block principal pivoting method for box-constrained quadratic programs,'' *Automatica*, vol. 100, pp. 29–37, Feb. 2019.

[37] M. Li, ''Generalized Lagrange multiplier method and KKT conditions with an application to distributed optimization,'' *IEEE Trans. Circuits Syst. II, Exp. Briefs*, vol. 66, no. 2, pp. 252–256, Feb. 2019.

ZHENG CHEN (Senior Member, IEEE) received the B.S. and M.S. degrees in electrical engineering and the Ph.D. degree in control science engineering from Northwestern Polytechnical University, Xi'an, China, in 2004, 2007, and 2012, respectively.

He was a Postdoctoral Fellow and a Research Scholar with the University of Michigan, Dearborn, USA, from 2008 to 2014. He is currently a Professor of Faculty of Transportation Engineering with the Kunming University of Science and Technology, Kunming, Yunnan, China. His research interests include predictive control, battery management systems, and energy management of hybrid electric vehicles. He has conducted more than 20 projects. He has published more than 80 peer-reviewed journal articles and conference proceedings. He was a recipient of Yunnan Oversea High Talent Project, China, and the Second Place of the IEEE VTS Motor Vehicles Challenge, in 2017 and 2018.

JIALUN CUI received the B.S. degree in vehicle engineering from the Kunming University of Science and Technology, Kunming, China, in 2018, where he is currently pursuing the M.S. degree in transportation engineering.

His research interest includes modeling and control of temperature control systems.

ZHENZHEN LEI received the M.S. degree in automotive system engineering from the University of Michigan-Dearborn, USA, in 2009, and the Ph.D. degree in automotive engineering from Chongqing University, China, in 2019.

She is currently a Lecturer of mechanical and power engineering with the Chongqing University of Science and Technology, Chongqing, China. She has published more than 15 peer-reviewed journal articles and conference proceedings. Her research interests include energy management of plug in hybrid electric vehicles and optimal control of intelligent electric vehicles.

JIANGWEI SHEN received the B.S. and M.S. degrees in traffic engineering, and power machine and engineering from the Kunming University of Science and Technology, Kunming, China, in 2008 and 2011, respectively, where he is currently pursuing the Ph.D. degree in automobile engineering.

He is currently an Experimentalist with the Kunming University of Science and Technology. His research interests include battery management systems and energy management of hybrid electric vehicles.

RENXIN XIAO received the B.S., M.S., and Ph.D. degrees in automation, control theory and control engineering, and mechanical design and theory from the Kunming University of Science and Technology, Kunming, China, in 2003, 2006, and 2013, respectively.

From 2006 to 2009, he worked for servo control as an Engineer with the Kunming Institute of Physics, Kunming. He is currently an Associate Professor of Faculty of Transportation Engineering with the Kunming University of Science and Technology. His research interests include temperature control, modeling of electric vehicle, battery management systems, and servo control of motor.